RESEARCH ARTICLE

A Novel Autologous CAR-T Therapy, YTB323, with Preserved T-cell Stemness Shows Enhanced CAR T-cell Efficacy in Preclinical and Early Clinical Development

Michael J. Dickinson[1], Pere Barba[2], Ulrich Jäger[3], Nirav N. Shah[4], Didier Blaise[5], Javier Briones[6], Leyla Shune[7], Nicolas Boissel[8], Attilio Bondanza[9], Luisa Mariconti[9], Anne-Laure Marchal[9], David S. Quinn[10], Jennifer Yang[10], Andrew Price[10], Akash Sohoni[10], Louise M. Treanor[10], Elena J. Orlando[10], Jennifer Mataraza[10], Jaclyn Davis[11], Darlene Lu[10], Xu Zhu[10], Boris Engels[10], Laure Moutouh-de Parseval[9], Jennifer L. Brogdon[10], Michele Moschetta[9], and Ian W. Flinn[12]

ABSTRACT CAR T-cell product quality and stemness (T_{stem}) are major determinants of *in vivo* expansion, efficacy, and clinical response. Prolonged *ex vivo* culturing is known to deplete T_{stem}, affecting clinical outcome. YTB323, a novel autologous CD19-directed CAR T-cell therapy expressing the same validated CAR as tisagenlecleucel, is manufactured using a next-generation platform in <2 days. Here, we report the preclinical development and preliminary clinical data of YTB323 in adults with relapsed/refractory diffuse large B-cell lymphoma (r/r DLBCL; NCT03960840). In preclinical mouse models, YTB323 exhibited enhanced *in vivo* expansion and antitumor activity at lower doses than traditionally manufactured CAR T cells. Clinically, at doses 25-fold lower than tisagenlecleucel, YTB323 showed (i) promising overall safety [cytokine release syndrome (any grade, 35%; grade ≥3, 6%), neurotoxicity (any grade, 25%; grade ≥3, 6%)]; (ii) overall response rates of 75% and 80% for DL1 and DL2, respectively; (iii) comparable CAR T-cell expansion; and (iv) preservation of T-cell phenotype. Current data support the continued development of YTB323 for r/r DLBCL.

SIGNIFICANCE: Traditional CAR T-cell manufacturing requires extended *ex vivo* cell culture, reducing naive and stem cell memory T-cell populations and diminishing antitumor activity. YTB323, which expresses the same validated CAR as tisagenlecleucel, can be manufactured in <2 days while retaining T-cell stemness and enhancing clinical activity at a 25-fold lower dose.

See related commentary by Wang, p. 1961.

INTRODUCTION

Chimeric antigen receptor (CAR) T-cell therapies directed against CD19 have demonstrated unprecedented efficacy in patients with different B-cell malignancies. Tisagenlecleucel, axicabtagene ciloleucel, and lisocabtagene maraleucel are approved for use in patients with relapsed/refractory (r/r) large B-cell lymphoma, including but not limited to diffuse large B-cell lymphoma (DLBCL; refs. 1–5). In this patient population, durable complete responses are observed only in 30% to 40% of cases, highlighting the need for more effective treatments to be developed (1, 2, 5).

Despite the remarkable efficacy of CAR T-cell therapies, many patients do not benefit from this treatment due to disease progression between leukapheresis and manufacturing/infusion, a failure to respond, or relapse after an initial response. Traditional CAR T-cell manufacturing requires extended culturing (≈10 days), which leads to a depletion of naive and stem cell memory T cells (T_{SCM}) in the final product (6). T_{SCM} have a unique stem cell–like ability to self-renew and the capacity to reconstitute the whole spectrum of memory and effector T (Teff)-cell subsets (7, 8). The longevity exhibited by T_{SCM} and the robust potential for immune reconstitution are associated with improved antitumor efficacy in adoptive T-cell transfer settings (8, 9). Similarly, recent preclinical studies have demonstrated improved antileukemic activity of CAR T cells manufactured without *ex vivo* activation and expansion (10) or after preselection of naive/T_{SCM} precursor cells (11).

CAR T cells from patients with chronic lymphocytic leukemia (CLL) who achieved a complete response have shown significantly higher expression of memory and early memory–related genes as compared with nonresponders (9). Importantly, a high frequency of naive and T_{SCM} cells in the leukapheresis material correlated with positive clinical outcomes in these patients. Based on these clinical observations and the fundamental idea that naive/T_{SCM} cells can persist and expand into a multifunctional pool of T cells in the patient, we sought to radically change the autologous CAR-T manufacturing process with the aim to retain these less-differentiated T-cell

[1]Clinical Haematology, Peter MacCallum Cancer Centre and Royal Melbourne Hospital, and the Sir Peter MacCallum Department of Oncology, University of Melbourne, Melbourne, Victoria, Australia. [2]Hematology Department, Hospital Universitari Vall d'Hebrón, Universitat Autònoma de Barcelona, Barcelona, Spain. [3]Clinical Division of Hematology and Hemostaseology, Department of Medicine I, and Comprehensive Cancer Center, Vienna General Hospital – Medical University of Vienna, Vienna, Austria. [4]Medical College of Wisconsin, Milwaukee, Wisconsin. [5]Département d'Hématologie, Programme de Transplantation et de Thérapie Cellulaire, Centre de Recherche en Cancérologie de Marseille, Aix-Marseille University, Institut Paoli Calmettes, Marseille, France. [6]Hematology Department, Hospital Santa Creu i Sant Pau, Barcelona, Spain. [7]University of Kansas Medical Center, Kansas City, Kansas. [8]Hematology Adolescent and Young Adult Unit, Saint-Louis Hospital, APHP, Paris, France. [9]Novartis Institutes for BioMedical Research, Basel, Switzerland. [10]Novartis Institutes for BioMedical Research, Cambridge, Massachusetts. [11]Novartis Pharmaceuticals Corporation, East Hanover, New Jersey. [12]Sarah Cannon Research Institute and Tennessee Oncology Center for Blood Cancers, Nashville, Tennessee.

Current address for A. Bondanza: AstraZeneca, Cambridge, United Kingdom; current address for B. Engels, Miltenyi Biotec, Bergisch Gladbach, Germany.

Prior presentation: Portions of this study were presented at the 2021 American Society of Hematology Annual Meeting and Exposition. Engels B, et al. *Blood* 2021;138(suppl 1): Abstract 2848, Flinn I, et al. *Blood* 2021; 138(suppl 1): Oral 740, and the 2022 European Hematology Association Hybrid Congress, Dickinson M, et al. EHA 2022; Abstract S212.

Corresponding Author: Michael J. Dickinson, Peter MacCallum Cancer Centre and Royal Melbourne Hospital, 305 Grattan Street, Melbourne VIC 3000, Australia. Phone: 61-38559-7858; Fax: 61-38672-0774; E-mail: Michael.Dickinson@petermac.org

Cancer Discov 2023;13:1982–97

doi: 10.1158/2159-8290.CD-22-1276

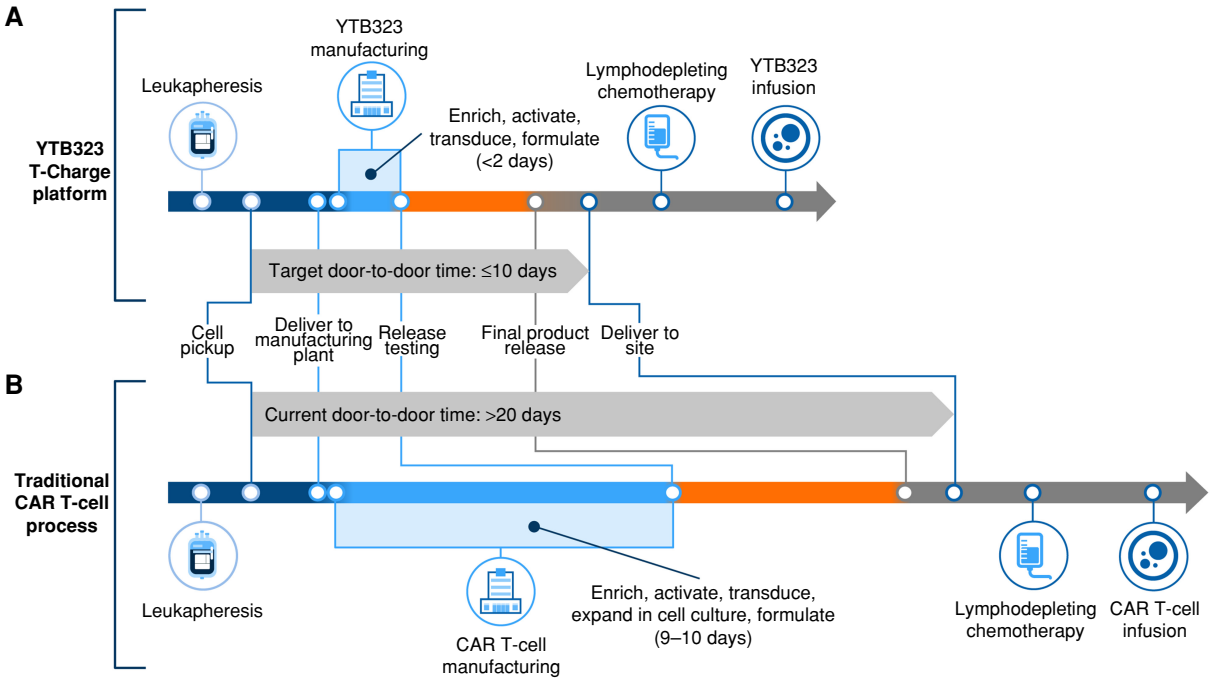

Figure 1. YTB323 vs. traditional CAR T-cell manufacturing. **A,** Using the novel T-Charge manufacturing platform, T cells are enriched from the patient's leukapheresis material, activated, and transduced with a lentiviral vector encoding the CD19-targeting CAR construct. After a short culture period, CAR-positive T cells are harvested, washed, and formulated in <2 days. Following successful clinical manufacturing, quality assurance assays (release testing) to assess cell viability, dose, and vector copy number are performed prior to final product release. Once manufactured in a commercial facility, YTB323 door-to-door time in the United States is anticipated to be 10 days or less. **B,** Using traditional manufacturing, T cells are enriched from the patient's leukapheresis material, activated, and transduced with a lentiviral vector encoding the CD19-targeting CAR construct. Following transduction, CAR T cells are expanded for 9 to 10 days before being washed and formulated. Following successful clinical manufacturing, quality assurance assays (release testing) to assess cell viability, dose, and vector copy number are performed prior to product release. Median door-to-door time for tisagenlecleucel has been reported at 20 or more days (25, 26). Door-to-door time is defined as the time from pickup of leukapheresis material to delivery of the final product back to the treatment site.

populations, enhance the potency of the product, and increase the scalability of the manufacturing process (4, 12).

Here, we present the preclinical development and the initial clinical evaluation of safety and preliminary antitumor efficacy of YTB323, a novel autologous CD19-directed CAR T-cell therapy manufactured utilizing a next-generation manufacturing process, in adult patients with r/r DLBCL after ≥2 lines of prior therapy (NCT03960840).

RESULTS

Preserved T-cell Stemness and Higher Expansion and Tumor Killing of YTB323 in Preclinical Models

YTB323 and CTL*019 (lab-grade tisagenlecleucel) CAR T cells were manufactured via isolation and activation of T cells in both processes, followed by gene transfer of the CAR via lentiviral transduction (Fig. 1A and B). For CTL*019, the cells were generated using the traditional CAR T-cell manufacturing process as previously described (13, 14). For YTB323, after gene transfer, the T cells were kept in culture for <2 days, and then washed and cryopreserved using the novel process known as T-Charge. The initial characterization of both YTB323 and CTL*019 products by flow cytometry demonstrated that YTB323 retained a higher percentage of naive/T_{SCM} cells ($CD45RO^-/CCR7^+$) from the input leukapheresis material compared with CTL*019—45.1% vs. 16.9%, respectively (Fig. 2A and B; Supplementary Fig. S1; ref. 13). In contrast, the traditional manufacturing process, which relies on prolonged *ex vivo* expansion, generated a final product that contained a much higher proportion of central memory T cells ($CD45RO^+/CCR7^+$) as opposed to naive/T_{SCM} cells.

Single-cell RNA sequencing (scRNA-seq) of YTB323 and CTL*019 products and leukapheresis starting material (input) was performed (13). YTB323 showed T_{SCM} and stemness gene signatures that closely resembled the starting material, while results for CTL*019 demonstrated decreased stemness with the concomitant increase in differentiation to effector memory T cells (Fig. 2C). Differential gene expression of CTL*019 cells versus YTB323 cells showed a significant overlap with T-cell differentiation pathways. Genes highly expressed in CTL*019 cells were associated with CD8 Teff cells and memory T cells compared with naive T cells, indicating that YTB323 cells were more naive-like compared with CTL*019 cells, which were more differentiated. Genes highly expressed in YTB323 cells were enriched for cytokine signaling pathways such as IL2 and IL12 signaling, as well as CD40 signaling. *BCL2L1*, the gene that codes for the antiapoptotic protein BCL-XL, was also upregulated in YTB323 compared with CTL*019 (Supplementary Fig. S2A–S2C) and is known to be upregulated in activated T cells upon CD3/CD28 stimulation (15).

The antitumor activity of YTB323 and CTL*019 was compared *in vitro* in a stress test using a repeat stimulation assay with the leukemia cell line NALM6 (Supplementary Fig. S3A). YTB323 cells were able to control the cancer cells at a 30-fold

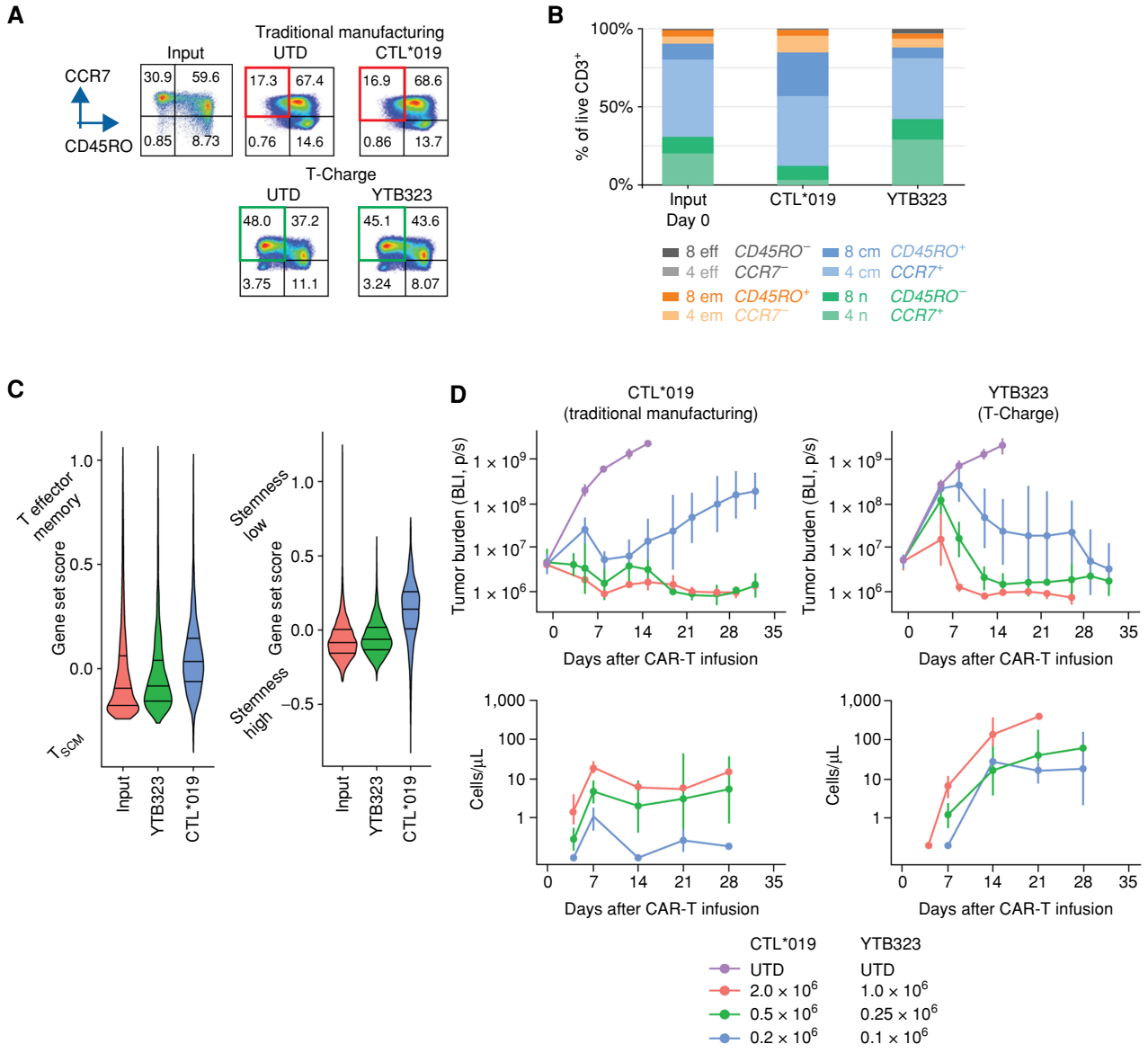

Figure 2. Preclinical evaluation and characterization of YTB323 and CTL*019. **A,** YTB323 and CTL*019 as well as untransduced T cells (UTD) were manufactured according to the traditional manufacturing and T-Charge processes, respectively. Data are representative of 3 full-scale runs with 3 different healthy donors ($n = 3$ healthy donors) performed in the preclinical setting. Phenotypic analysis of leukapheresis (input) and CAR-T products after thaw of the cryopreserved product. Gating on live CD3⁺ events used to determine T-cell subsets (CCR7 vs. CD45RO). Numbers in quadrants indicate the percentage of the parental CD3⁺ population. Extended culture of T cells *ex vivo*, such as in traditional manufacturing, leads to a loss of T_{SCM} and naive phenotypes (red boxes). In contrast, limited culture *ex vivo* allows for the maintenance of naive-like cells by the T-Charge process (green boxes). **B,** Composition of YTB323 and CTL*019 is shown for the CD3⁺ population of donor 1 (donor 2 and 3 compositions can be found in Supplementary Fig. S1). The percentage (%) of the respective populations (colors) refers to the percentage of CD3⁺ T cells. 4 and 8, CD4⁺ and CD8⁺, respectively; cm, central memory; eff, effector; em, effector memory; n, naive-like. **C,** Single-cell gene set enrichment for input (leukapheresis), YTB323, and CTL*019 cells. Gene signature sets for T effector memory compared with T stem cell memory (left; ref. 7) cells and stemness (right; ref. 36) were assessed for gene set enrichment in each cell in the 3 samples. Violin plots compare the gene set enrichment scores between the 3 samples, with lines indicating the 25%, 50%, and 75% quantiles. Data shown are derived from 1 healthy donor. **D,** Top: NSG mice were injected with the pre–B-acute lymphoblastic leukemia line NALM6, expressing the luciferase reporter gene; the tumor burden is expressed as total body luminescence (BLI, p/s), depicted as mean tumor burden with 95% confidence interval (CI). On day 7 after tumor inoculation, mice were treated with YTB323 or CTL*019 at the respective doses (number of viable CAR⁺ T cells). The high-dose YTB323 group was terminated on day 33 due to the onset of xenogeneic graft-versus-host disease. UTD served as negative control. $n = 5$ mice for all groups, except $n = 4$ for T-Charge UTD, 1×10^6 dose, and all CTL*019 dose groups. Five xenograft studies were run with CAR T cells generated from 5 different healthy donors, 3 of which included a comparison with CTL*019. Bottom: Time course of CAR⁺ T-cell concentration in NALM6 tumor–bearing mice treated with UTD, CTL*019, or YTB323 at 3 respective doses. Blood samples were taken at 4, 7, 14, 21, and 28 days after CAR-T injection. CAR⁺ T-cell (CD3⁺CAR⁺) concentrations were analyzed by flow cytometry at designed time points, depicted as mean cells with 95% CI. Reprinted from *Blood*, 138 (suppl 1), Engels B, et al. Preservation of T-cell stemness with a novel expansionless CAR-T manufacturing process, which reduces manufacturing time to less than two days, drives enhanced CAR-T cell efficacy, Abstract 2848, Copyright © 2021, with permission from American Society of Hematology. Published by Elsevier Inc. All rights reserved (13).

Table 1. Baseline demographic and disease characteristics by dose level

	All patients ($N = 20$)	
	DL1 (2.5×10^6) $n = 4$	DL2 (12.5×10^6) $n = 16$
Median age (range), years	69 (60–74)	66 (41–78)
≥65 y, *n* (%)	2 (50)	9 (56)
ECOG PS, *n* (%)		
0	4 (100)	11 (69)
1	0	5 (31)
Stage at study entry, *n* (%)		
I	2 (50)	2 (13)
II	0	2 (13)
III/IV	2 (50)	12 (75)
Lines of prior therapies, *n* (%)		
2	2 (50)	11 (69)
>2	2 (50)	5 (31)
Elevated LDH,[a] *n* (%)	2 (50)	8 (50)
Prior autologous HSCT, *n* (%)	1 (25)	6 (38)

Abreviations: DL, dose level; ECOG PS, Eastern Cooperative Oncology Group performance status; HSCT, hematopoietic stem cell transplant; LDH, lactate dehydrogenase.

[a]Varies depending on the upper limit of normal for each site.

lower effector:tumor cell ratio and suppressed cancer outgrowth for ≥5 stimulations compared with CTL*019 cells. So that the capacity of YTB323 to secrete cytokines could be assessed, cocultures were set up with cancer cell lines, and cytokines were measured after 24 or 48 hours of coculture at a 1:1 effector:target ratio. Compared with CTL*019, YTB323 T cells exhibited 11- to 17-fold higher levels of IFNγ (Supplementary Fig. S3B) and 3.5- to 10-fold higher levels of IL2 (Supplementary Fig. S3C) secretion upon coculture with cells from the DLBCL cell line (TMD8) or from the leukemia cell line (NALM6), respectively. YTB323 T cells showed low background levels of cytokine secretion after a 24-hour rest period while retaining CD19-specific activation and cytokine secretion (Supplementary Fig. S3D and S3E).

Antitumor efficacy of YTB323 against B-cell tumors *in vivo* was assessed, in a range of doses, in immunodeficient NOD-scid gamma (NSG) mice engrafted with the leukemia cell line NALM6 and the DLBCL cell line TMD8. At high CAR T-cell doses, both YTB323 and CTL*019 were able to fully eradicate the NALM6 leukemia cells and TMD8 DLBCL cells. YTB323 controlled NALM6 B-cell acute lymphoblastic leukemia (B-ALL) tumor growth at a low dose of only 0.1×10^6 CAR^+ viable T cells compared with 0.5×10^6 CAR^+ viable T cells required for CTL*019 (Fig. 2D; ref. 13). Due to the robust expansion of YTB323 cells, early graft-versus-host disease was observed in animals infused with YTB323 cells in the NALM6 model and the study had to be concluded at 28 days.

YTB323 expansion ability was examined through comparison with CTL*019 in these tumor-bearing mice. *In vivo* expansion of CAR^+ T cells in blood was analyzed weekly by flow cytometry for up to 4 weeks after infusion (Fig. 2D; ref. 13). Dose-dependent maximal expansion (C_{max} and $AUC_{0\text{–}21d}$) was observed for both YTB323 and CTL*019. Given the same dose, a 50-times higher C_{max} and 30-times higher $AUC_{0\text{–}21d}$ were observed for YTB323 compared with CTL*019 (Supplementary Fig. S4). YTB323 time to peak expansion (T_{max}) was delayed by at least 1 week compared with CTL*019. The preclinical data obtained for YTB323 demonstrated that the preservation of T-cell stemness with the new manufacturing process generated a product with higher expansion and tumor-killing potency, warranting further exploration in patients in a phase I clinical trial.

YTB323 First-in-Human Trial: Design and Initial Data in R/R DLBCL Patients

Based on the preclinical findings, a first-in-human study of YTB323 was initiated, aimed to characterize safety, feasibility, and cellular kinetics, to identify a recommended dose and to assess preliminary evidence of efficacy in patients with r/r DLBCL, r/r CLL, and adult r/r ALL. Here, we report interim data in patients with r/r DLCBL. Dose escalation was ongoing as per this manuscript data cutoff, and a recommended dose had not yet been identified. As of August 20, 2021, 27 patients with r/r DLBCL had been enrolled, two patients were not infused (one death, one product-related issues), two were pending infusion, three patients were enrolled at dose level 3 (not included in this analysis), and 20 patients received YTB323 according to the trial study design [Methods; four patients at dose level 1 (DL1) and 16 patients at dose level 2 (DL2)]. All patients at DL1 received the target dose of 2.5×10^6 CAR^+ viable YTB323 T cells. Fourteen of the 16 patients at DL2 received the target dose of 12.5×10^6 CAR^+ viable YTB323 T cells; two patients received 6.8×10^6 and 7.4×10^6 CAR^+ viable YTB323 T cells, respectively. These doses reflect values 10 to 50 times lower than the typical tisagenlecleucel dose range of 60×10^6 to 600×10^6 CAR^+ viable cells for patients with r/r DLBCL (4).

At the study entry, the median age among patients treated with YTB323 was 65 years (Table 1)—approximately 10 years older than the median age of patients in the JULIET trial (56 years; ref. 4). At DL1 and DL2, 50% and 75% of patients had

Table 2. Overall safety profile by dose level of YTB323

	DL1 (2.5×10^6) $n = 4$		DL2 (12.5×10^6) $n = 16$	
	Any grade *n* (%)	Grade ≥3 *n* (%)	Any grade *n* (%)	Grade ≥3 *n* (%)
Adverse events				
Any AE[a]	4 (100)	4 (100)	16 (100)	12 (75)
Death[b]	2 (50)	2 (50)	3 (19)	3 (19)
Related to YTB323	0		0	
Infections	2 (50)	1 (25)	3 (19)	1 (6)
CRS[c]	1 (25)	0	5 (31)	1 (6)
Neurologic AR	1 (25)	0	4 (25)[d]	1 (6)
Hematology laboratory abnormalities after YTB323 treatment				
Any cytopenia[e]	4 (100)	4 (100)	16 (100)	16 (100)
Anemia	4 (100)	4 (100)	16 (100)	7 (44)
Leukopenia	4 (100)	3 (75)	16 (100)	14 (88)
Lymphopenia	4 (100)	3 (75)	16 (100)	16 (100)
Neutropenia	4 (100)	4 (100)	16 (100)	14 (88)
Thrombocytopenia	4 (100)	2 (50)	16 (100)	8 (50)

NOTE: MedDRA v24.0 and CTCAE v5.0 were used for the reporting of AEs.

Abbreviations: AE, adverse event; AR, adverse reaction; CRS, cytokine release syndrome; CTCAE, Common Terminology Criteria for Adverse Events; DL, dose level; ICANS, immune effector cell–associated neurotoxicity syndrome; MedDRA, Medical Dictionary for Regulatory Activities.

[a]All AEs were reported regardless of the study drug relationship.

[b]Three deaths were due to disease progression (1 at DL1, 2 at DL2), 1 was due to intestinal hemorrhage (at DL2), and 1 was due to sepsis (at DL1).

[c]Grading of CRS according to Lee et al. (16) criteria.

[d]One patient experienced a grade 2 seizure that constituted grade 3 ICANS, and 1 other patient experienced grade 3 ICANS.

[e]Reported regardless of study drug relationship.

stage III or IV disease, respectively. At both DL1 and DL2, 50% had elevated levels of lactate dehydrogenase (>the upper level of normal). All patients received ≥2 lines of prior therapy, including 25% of DL1 patients and 38% of DL2 patients who received prior autologous hematopoietic stem cell transplant (HSCT). Patients at DL1 had received a median of 2.5 (range, 2–4) lines of prior therapies. Patients at DL2 received a median of 2 (range, 2–7) lines of prior therapies. Bridging therapy given after leukapheresis at the investigator's decision was received by 75% of patients in each dose level (Supplementary Table S1); all patients, except one at DL1, received lymphodepleting chemotherapy (fludarabine and cyclophosphamide) prior to YTB323 infusion (Supplementary Table S2).

YTB323 Has a Manageable Safety Profile

All 20 patients were included in the safety analysis: four patients at DL1 and 16 patients at DL2 (Table 2; ref. 16). Any-grade adverse events (AE) were reported in all patients at DL1 and DL2. Grade ≥3 AEs were reported in four (100%) patients at DL1 and 12 (75%) patients at DL2. Cytopenias were reported in all patients at DL1 and DL2 (Table 2; ref. 16). There were two (50%) deaths at DL1 and three (19%) at DL2, of which none was considered treatment related. At DL1, one death was due to sepsis (day 59) and one was due to disease progression (day 268). At DL2, one death was due to intestinal hemorrhage (day 62) and two were due to disease progression (days 281 and 139).

Cytokine release syndrome (CRS) was reported as generally low grade according to Lee and colleagues (16) and the American Society for Transplantation and Cellular Therapy (ASTCT; ref. 17) criteria. The median (range) time to onset of CRS was 9 (9–9) and 11 (1–17) days for patients at DL1 and DL2, respectively (Supplementary Table S3), which is later than what is typically seen with most CAR-T products that use *in vitro* expansion (4, 18, 19). Six patients (30%) experienced CRS at DL1 and DL2. Five (25%) patients had grade 1/2 CRS, and one (5%) patient experienced grade 4 CRS at DL2, which met protocol-defined dose-limiting toxicity (DLT) criteria. At DL1, no patient received tocilizumab or corticosteroids for CRS management. At DL2, four (25%) patients received tocilizumab, two (12.5%) of whom received a combination of tocilizumab and corticosteroids. The median time to CRS resolution was 5 days at DL1 and 2 days at DL2.

Most of the neurologic adverse reactions (NAR) reported following YTB323 treatment were grade 1 according to Common Terminology Criteria for Adverse Events (CTCAE) v5.0 (Supplementary Table S4). Grade ≥3 NAR were reported in one (25%) patient at DL1 and one (6%) patient at DL2. The median time to onset of NAR was 7 and 6.5 days for DL1 and DL2, respectively. The median time to NAR resolution was 5 days at DL1 and 14 days at DL2. Immune effector cell–associated neurotoxicity syndrome (ICANS) following YTB323 infusion was reported in two (12.5%) patients at DL2; both patients experienced grade 3 ICANS.

YTB323 Shows Encouraging Efficacy in R/R DLBCL Patients

Nineteen patients were evaluable for efficacy after YTB323: four patients at DL1 and 15 patients at DL2 (Fig. 3A; ref. 20).

A

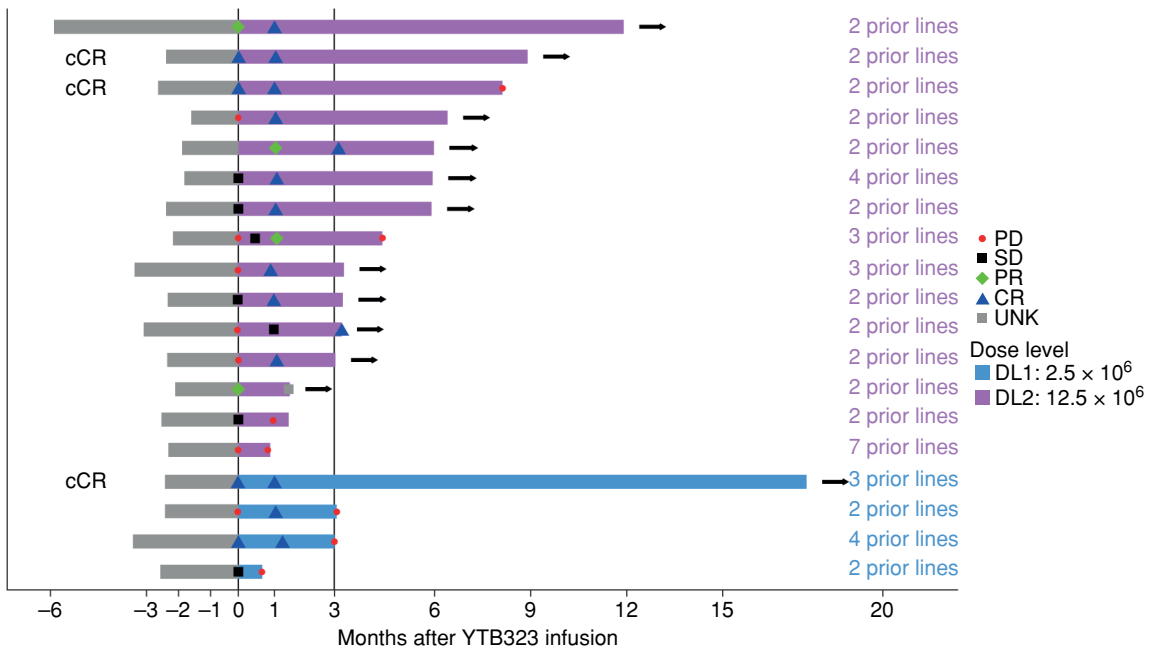

B

	Patients evaluable for efficacy at month 3 (N = 19)	
	DL1 (n = 4)	DL2 (n = 15)
CR at month 3, n (%)	1 (25)	11 (73)
CR at last assessment before YTB323,[a] n (%)	1 (25)	2 (13)
PR, n (%)	0	0
SD, n (%)	0	0
PD, n (%)	3 (75)	2 (13)
Unknown	0	2 (13)

Figure 3. Efficacy of YTB323 in patients with r/r DLBCL. **A,** Swimmer plot of YTB323 efficacy in patients with r/r DLBCL. Nineteen patients with r/r DLBCL were infused with YTB323 and evaluable for efficacy. Three patients at DL1 and 12 at DL2 responded to YTB323. Five patients at DL2 had high lactate dehydrogenase (LDH) at baseline (rows 4, 6, 8, 13, and 15 from the top), 7 patients at DL2 had high LDH at screening (rows 2, 4, 6–8, 14, and 15 from the top), and 4 patients had elevated LDH at both baseline and screening (rows 4, 6, 8, and 15 from the top). At DL1, 2 patients had high LDH at baseline (rows 18 and 19 from the top), 2 patients had high LDH at screening (rows 17 and 19 from the top), and 1 patient had elevated LDH at both baseline and screening (row 19 from the top). Arrow denotes ongoing efficacy assessments. Gray bars represent screening prior to infusion; purple bars represent screening after infusion. The symbols at time 0 represent each patient's disease status at the time of YTB323 infusion. **B,** Complete response rate following YTB323 treatment. [a]Patients who were in CR prior to receiving YTB323 due to either a late effect of prior therapies or bridging chemotherapy. cCR, continuous CR indicates patients in CR before infusion of YTB323; DL, dose level; PD, progressive disease; SD, stable disease; UNK, unknown. Panel A reprinted from *Blood*, 138 (suppl 1), Flinn I, et al. A first-in-human study of YTB323, a novel, autologous CD19-directed CAR-T cell therapy manufactured using the novel T-charge TM platform, for the treatment of patients (pts) with relapsed/refractory (r/r) diffuse large B-cell lymphoma (DLBCL), 2021; Oral 740. Copyright © 2021 American Society of Hematology. Published by Elsevier Inc. All rights reserved (20).

At a median follow-up of 14 months for DL1 and 6 months for DL2, patients experienced an overall response rate (ORR) of 75% and 80%, respectively. At month 3, one (25%) patient at DL1 and 11 (73%) at DL2 achieved a complete response (CR). Of note, at DL1 and DL2, respectively, two (50%) and two (13%) patients were in CR prior to YTB323 administration at their last assessment after bridging chemotherapy. Among the patients who achieved a response [CR/partial response (PR)] at DL1 and DL2, 1/3 (33%) and 10/12 (83%) did not experience disease progression after a median follow-up of 14.0 months and 6.2 months, respectively (Fig. 3B). Given the short duration of follow-up, progression-free and overall survival (OS) analyses could not provide definitive conclusions.

Pharmacokinetics Demonstrate Enhanced Proliferative Potential of YTB323

Cellular kinetics of YTB323 in patients was assessed as a secondary endpoint (Fig. 4A). Although moderate-to-high

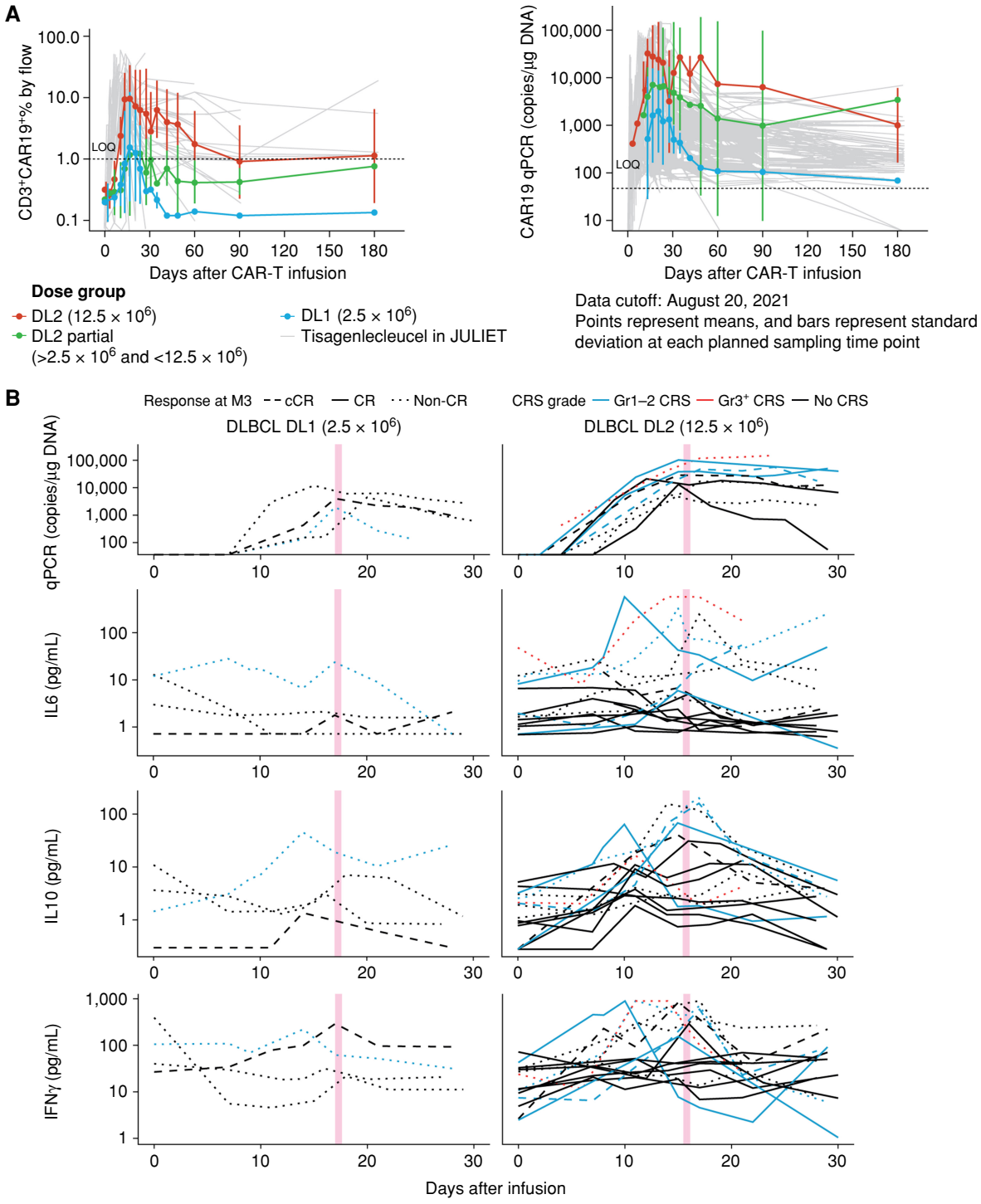

Figure 4. Cellular kinetics of YTB323 and cytokine profiles. **A,** Cellular kinetics profile of YTB323 assessed by flow cytometry (left) and qPCR (right) up to 90 days overlaid with tisagenlecleucel data (JULIET) in patients with r/r DLBCL. Left: CAR expression by flow cytometry, as a percentage of $CD3^+CAR19^+$ cells in $CD3^+$ cells, after YTB323 infusion in patients who received full DL1 (2.5×10^6 cells) are presented in blue, below target DL2 ($>2.5 \times 10^6$ and $<12.5 \times 10^6$ cells) in green, and full DL2 (12.5×10^6 cells) in red; CAR expression by flow cytometry after tisagenlecleucel infusion ($0.1–6.0 \times 10^6$ cells; median, 3.0×10^6 cells) is presented in gray. Right: CAR transgene levels by qPCR, as copies/µg DNA, after YTB323 infusion in patients who received full DL1, are presented in blue, partial DL2 in green, and full DL2 in red; CAR transgene levels by qPCR after tisagenlecleucel infusion are presented in gray. **B,** Cytokine profiles following YTB323 infusion. IL6, IL10, and IFNγ were measured by mean square displacement analysis up to 30 days for patients with cCR (long dashed line), CR (solid line), and non-CR (short dashed line), and with no CRS (black), grade (Gr) 1–2 CRS (blue), and Gr >3 CRS (red). Pink bar indicates the median time of peak expansion measured by qPCR as in **A**. cCR, continuous CR indicates patients in CR before infusion of YTB323; CD, cluster of differentiation; DL, dose level; IFNγ, interferon gamma; IL, interleukin; LOQ, limit of quantification; qPCR, quantitative polymerase chain reaction.

variability in kinetics was observed, which may be due to patient disease condition, leukapheresis material differences, and the small sample size, YTB323 exposure (C_{max} and $AUC_{0–28d}$) at DL2 was higher than that at DL1 (Supplementary Tables S5 and S6). Overall exposure at DL2 was comparable with that of tisagenlecleucel, however, at a 25-fold lower median dose in patients with DLBCL (21). Both the time to reach peak expansion (T_{max}) as measured by flow cytometry and the onset of CRS showed a delay compared with tisagenlecleucel: T_{max} of 16 days with YTB323 versus 9 days in JULIET and 10 days to CRS onset with YTB323 versus 3 days in JULIET (4). This is consistent with the observation in preclinical models. The T_{max} of YTB323 also coincided with the peak concentration of most cytokines (Fig. 4B). Long-term persistence data are still emerging. Nevertheless, at DL2, CAR expression was detectable in three of seven evaluable patients at 6 months and detectable for at least 9 months by flow cytometry.

YTB323 Product Exhibits Preservation of T-cell Subpopulation Distribution and Stemness Compared with Tisagenlecleucel

Accompanying the promising clinical efficacy of YTB323, several exploratory endpoints were aimed at better understanding the effect of the new manufacturing process on CAR T-cell product characteristics. Both flow cytometry and RNA-seq assessments suggested that the new manufacturing process preserved the cellular characteristics of the leukapheresis material in the YTB323 final product. The CD4:CD8 ratio in the leukapheresis material remained consistent in the YTB323 final product, whereas a marked increase in the CD4:CD8 ratio was observed in the tisagenlecleucel final product (Supplementary Fig. S5). Minimal changes in the percentages of CD4 and CD8 naive/T_{SCM} cell ($CD45RA^+/CCR7^+$) phenotypes were observed when comparing the leukapheresis material to the YTB323 final product [CD4: −6.14% (range, −10.98 to −1.31); CD8: −4.57% (range, −9.18 to 0.03)] by flow cytometry (Fig. 5A). By contrast, decreases in both CD4 and CD8 naive/T_{SCM} cells were observed between the leukapheresis material and the tisagenlecleucel final product from patients enrolled in the JULIET clinical trial [CD4: −12.3% (range, −14.5 to −10.2); CD8: −10.9% (range, −13.9 to −7.8); Fig. 5B]. In addition, marked decreases in Teff cells ($CD45RA^+/CCR7^-$) were observed in the tisagenlecleucel final product; although this population was not directly measured in the YTB323 product, an analogous population of senescent/exhausted T cells ($CD27^-CD28^-$) was comparable between leukapheresis material and the YTB323 final product.

Bulk RNA-seq and scRNA-seq analyses confirmed that YTB323 retained a stem-like gene signature (Fig. 5C, refs. 7, 22; Supplementary Fig. S6, refs. 7, 23, 24) compared with the leukapheresis material, recapitulating what was observed in the preclinical studies. By contrast, tisagenlecleucel product cells exhibited greater differentiation from naive/early memory T cells to effector/late memory T cells, with a significant decrease in stemness compared with the leukapheresis material. Evaluation of commercial tisagenlecleucel versus YTB323 final products using differential gene expression analysis confirmed that tisagenlecleucel cells highly expressed genes associated with the G_2–M cell-cycle stage, CD8 Teff cells, and regulatory T cells (Treg). These findings indicate that YTB323 cells were more stem-like and at an earlier stage of differentiation compared with CTL*019 cells, which are more differentiated and associated with Tregs. Genes highly expressed in YTB323 cells were enriched for cytokine signaling pathways such as IL2, IL23, IL27, and CD40, as well as hematopoietic stem cell–associated genes (Supplementary Fig. S7A–S7C). *BCL2L1* gene expression was downregulated in tisagenlecleucel from the JULIET study compared with YTB323, recapitulating the observation in the preclinical studies (Supplementary Fig. S7A).

Flow cytometry and scRNA-seq revealed that a higher baseline immune competence may enhance YTB323 activity. scRNA-seq of the input leukapheresis from patients receiving YTB323 showed that patients with a CR had higher levels of natural killer and CD4 central memory T cells, whereas patients with progressive disease (PD) had higher levels of CD8 effector memory T cells and monocytes, particularly monocytes expressing myeloid-derived suppressor cell–associated genes (Supplementary Fig. S8A; ref. 23). Similarly, flow cytometry of the $CD3^+$ T cells in the leukapheresis material showed higher levels of naive/T_{SCM} and central memory T cells in patients with a CR, whereas patients with PD had higher levels of senescent/exhausted T cells and effector memory T cells (Supplementary Fig. S8B).

These differences in T-cell states in the leukapheresis between response groups were maintained in the final product (Supplementary Fig. S8C and S8D). For example, the final products of patients with CR continued to have higher central memory and naive T cells, as measured by both scRNA-seq and flow cytometry, whereas those of patients with PD continued to have higher levels of effector memory and exhausted T cells. scRNA-seq in the final product also showed a correlation between T-cell stemness characterization and peak expansion ($R^2 = 0.61$; Supplementary Fig. S8E).

Figure 5. T-cell phenotype of CD4 and CD8 subsets in leukapheresis and YTB323 and tisagenlecleucel final products. **A,** Left: T-cell memory subsets in the leukapheresis ($n = 17$) preserved in the YTB323 final product ($n = 16$) using flow cytometry. Phenotype percentages of CD4 or CD8 for paired patient samples: naive/T_{SCM} = $CCR7^+CD45RA^+$; central memory = $CCR7^+CD45RO^+$, effector memory = $CCR7^-CD45RO^+$, and senescent/exhausted = $CD27^-CD28^-$. Right: Absolute changes in phenotype frequencies [mean difference and 95% confidence interval (CI)] show overall preservation of memory T-cell subsets. **B,** Left: Significant changes in T-cell memory subsets between the leukapheresis ($n = 122$) and tisagenlecleucel final product ($n = 140$), including lower frequency of naive/T_{SCM} in the final product using flow cytometry. Phenotype percentages of CD4 or CD8 for paired patient samples: naive/T_{SCM} = $CCR7^+CD45RA^+$, central memory = $CCR7^+CD45RA^-$, effector memory = $CCR7^-CD45RA^-$, and effector = $CCR7^-CD45RA^+$. Right: Absolute changes in phenotype frequencies (mean difference and 95% CI) show significant shifts in memory T-cell subsets between the leukapheresis and final product. Leukapheresis material and tisagenlecleucel final product were from patients enrolled in the JULIET clinical trial (NCT02445248). **C,** YTB323 retains a naive stem-like gene signature. Single-sample gene set enrichment for leukapheresis and cell product T cells from bulk RNA-seq. YTB323: <2-day manufacturing with T-Charge platform. Tisagenlecleucel: standard 9-day tisagenlecleucel manufacturing. Gene signature sets for stemness (left; ref. 22) and naive T cells (Tn) vs. effector memory T cells (TEM; right; ref. 7) were assessed for gene set enrichment scores in the leukapheresis and YTB323 and tisagenlecleucel cell products. *P* values are calculated for the comparison of YTB323 leukapheresis ($n = 12$) vs. cell products ($n = 11$) and tisagenlecleucel leukapheresis ($n = 9$) vs. cell products ($n = 23$).

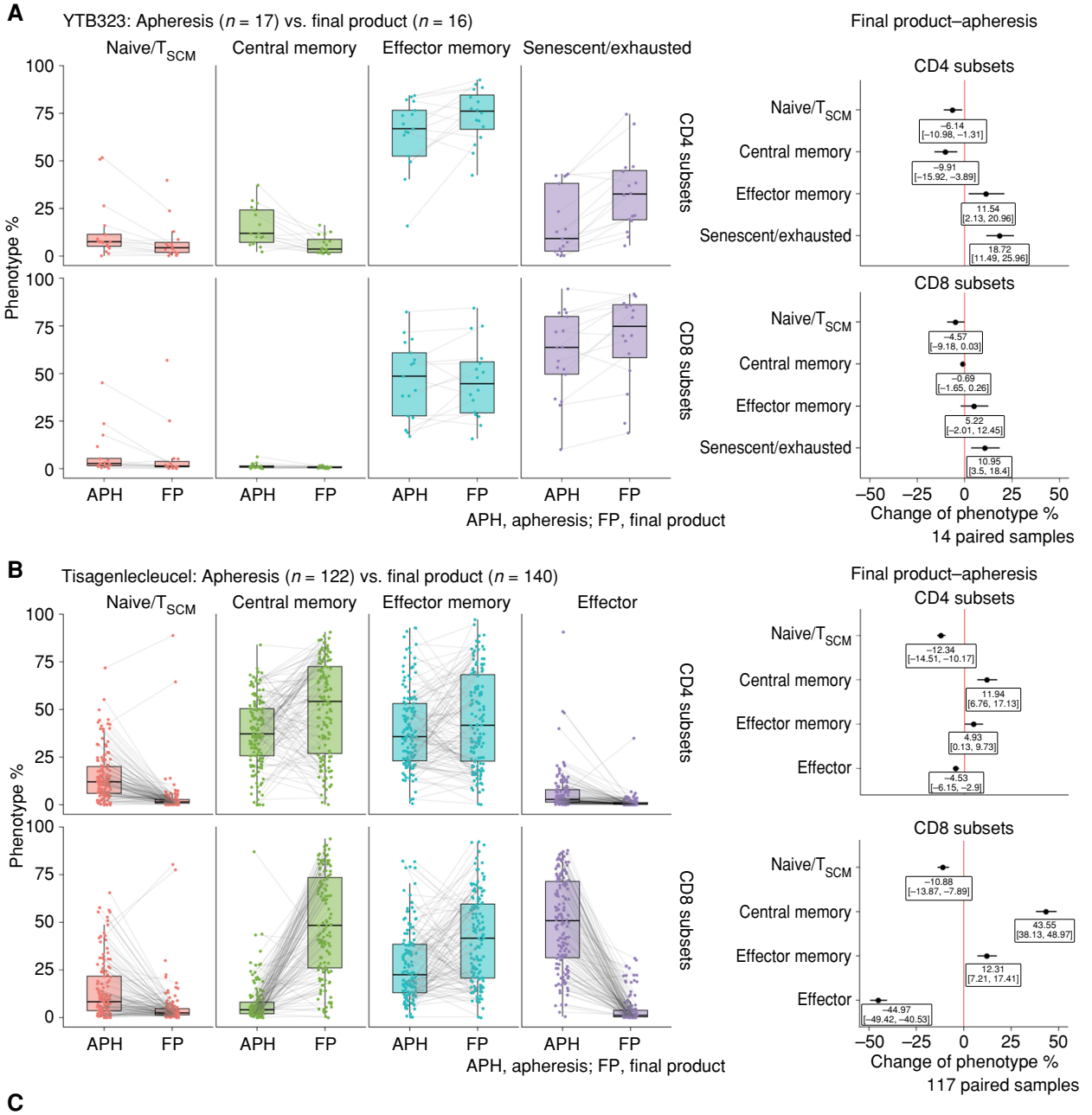
A
YTB323: Apheresis (n = 17) vs. final product (n = 16)
Naive/T_SCM
Central memory
Effector memory
Senescent/exhausted
CD4 subsets
CD8 subsets
Phenotype %
APH
FP
APH, apheresis; FP, final product
Final product–apheresis
Change of phenotype %
14 paired samples
B
Tisagenlecleucel: Apheresis (n = 122) vs. final product (n = 140)
Effector
117 paired samples
C
0.032
0.00051
0.17
1.8e–08
High stemness
Low stemness
Stemness gene set score
Naive T cells
Effector memory T cells
Tn vs. TEM gene set score
Leukapheresis
Product
YTB323
Tisagenlecleucel
Product
Tisagenlecleucel
YTB323

To examine the immune phenotype of the YTB323 product during the peak expansion phase, flow cytometric analyses were performed on post-YTB323 infusion samples (on days 14, 17, 21, and 28). Patients achieving a CR at month 3 had higher levels of CD4 and CD8 effector memory T cells during this expansion phase from day 14 to day 28 as compared with patients with PD. Patients with PD had higher levels of CD4 and CD8 senescent/exhausted T cells in the YTB323 product and at multiple postinfusion time points (Supplementary Fig. S9A). An increase in PD-1 staining was observed on both CD4 and CD8 T cells in all patients starting on day 14. However, patients with PD had higher levels of TIM-3$^+$ and TIM-3$^+$PD-1$^+$ CD4 and CD8 cells at several postinfusion time points as compared with patients who achieved a CR (Supplementary Fig. S9B).

DISCUSSION

Here, we describe the initial development of YTB323, a novel autologous CD19 CAR-T therapy, which is manufactured utilizing an innovative approach aimed at preserving T-cell stemness. YTB323 utilizes the same CAR construct as tisagenlecleucel, offering the unique opportunity to compare two CAR T-cell therapies that differ only in the way that the CAR T cells are manufactured.

The preclinical development and validation studies presented here demonstrate that YTB323, which has an optimal manufacturing process time of <2 days, retained the naive and T_{SCM} content of the input leukapheresis material. When tested *in vitro*, YTB323 demonstrated better killing capability upon repetitive stimulation as compared with traditionally manufactured CAR T cells. Further, YTB323 exhibited enhanced *in vivo* expansion and higher potency, as shown by tumor eradication at lower doses in NSG models. Similarly, a recent preclinical study demonstrated that preselection of naive/T_{SCM} precursor cells leads to increased potency and higher T-cell expansion, which was ultimately associated with a safer preclinical profile (11). These preclinical observations were recapitulated in patients treated with YTB323 in the present phase I study. A striking preservation of T-cell stemness and T-cell subset distribution in the final product was demonstrated by both flow cytometry and gene expression analyses at the single-cell level. Studies have shown that T_{SCM} cells are a less-differentiated population of cells that have enhanced proliferative and survival capacity compared with other T-cell subpopulations (e.g., central memory and Teff; ref. 7). Such preservation of T-cell stemness in the product also translates into promising early clinical activity with a desirable safety profile.

In patients with r/r DLBCL, YTB323 demonstrated efficacy across DL1 and DL2, with an ORR of 75% and 80%, respectively. Interestingly, at month 3, 73% of patients infused with YTB323 at DL2 achieved a CR, and only two of 15 (13%) patients at DL2 progressed after obtaining a CR/PR with a median follow-up of 6 months. Although four patients achieved CR after bridging therapy and prior to YTB323 infusion, the durability of the response is unlikely due to the single cycle of bridging chemotherapy alone, but the lower disease burden may have contributed to the durable benefits from YTB323. Taken together, these data suggest YTB323 may be effective at controlling disease progression in patients with r/r DLBCL.

Higher *in vivo* expansion of YTB323 at DL2 compared with DL1 is observed in patients with r/r DLBCL. YTB323 is effective with comparable *in vivo* CAR-T exposure (C_{max} and $AUC_{0–28d}$) to tisagenlecleucel in patients with DLBCL, at a 25-fold lower median dose (DL2 of YTB323 at 12.5×10^6 cells vs. tisagenlecleucel at 300.0×10^6 cells in the JULIET study; ref. 21), confirming its capacity for expansion and its potency. Long-term data on YTB323 persistence in the peripheral circulation are still emerging. Current CAR T-cell therapies produced by traditional manufacturing are administered at high doses (0.6 to 6×10^8 CAR$^+$ viable T cells for tisagenlecleucel) and infused as a bolus of differentiated CAR T cells, which could contribute to the incidence of acute CRS. Infusing a substantially lower dose (2.5 to 12.5×10^6 CAR$^+$ viable T cells) of potent YTB323 cells allows progressive expansion within the patient, with a delayed T_{max}, and potentially slower release of cytokines in the systemic circulation and reduced severity of CRS (11). Of note, CRS reported in patients treated with YTB323 was generally low grade, had a later onset than is typically observed with other CAR-T therapies, and correlated well with the delayed peak of expansion, as shown in Fig. 4 (median T_{max}, 16 vs. 9 days for tisagenlecleucel). It will be important to monitor the safety of YTB323 in a larger number of patients to determine if this new manufacturing process, the lower dose, and the different cell expansion kinetics result in a favorable safety profile and lower incidence of CRS as compared with tisagenlecleucel. Overall, this preliminary efficacy data at DL2 show potentially improved activity of YTB323 as compared with tisagenlecleucel (4), with a favorable safety profile at a considerably lower dose.

This interim analysis of the DLBCL cohort from the phase I dose-escalation trial was designed to investigate the safety, feasibility, and efficacy of YTB323, which was manufactured in a pilot manufacturing facility and therefore did not evaluate manufacturing turnaround time. Turnaround time (door-to-door time), which includes the time from pickup of leukapheresis material to return of the product to the hospital, can vary for any CAR T-cell product depending on logistics and location of the clinical site. In addition, the time needed for CAR T-cell quality assurance testing to determine cell viability, dose, vector copy number, and sterility can also affect door-to-door time for any product. During the YTB323 phase I trial, sterility testing was significantly shortened and will be further optimized as YTB323 moves into phase II development and beyond. It is an anticipated goal that commercial manufacturing facilities will achieve a door-to-door time of 10 days or less in the United States (Fig. 1). Traditional manufacturing processes have been reported at a median of >20 days for tisagenlecleucel (25, 26). It is important to remember that vein-to-vein time of any CAR T-cell product, the time from leukapheresis to infusion, can vary based on the clinical management of each patient, which is at the direction of the treating physician and beyond the scope of manufacturing.

Another limitation of this interim analysis is the currently reported clinical sample size ($N = 20$). However, the study is ongoing, and a larger patient population is being evaluated. In a more recent data cut (March 31, 2022), outcomes in

45 patients with DLBCL across four dose levels (2.5×10^6, 12.5×10^6, 25×10^6, 40×10^6 CAR$^+$ viable T cells) were assessed. Based on the CR rate at 3 months (63%), favorable safety profile, and cellular kinetics, DL2 was determined to be the recommended phase III dose (27). The tisagenlecleucel CAR transgene and autologous cell therapy have been proven to be highly effective in adult patients with r/r DLBCL. Improving T-cell fitness to enhance CAR T-cell potency is a core component of the next-generation manufacturing platform termed T-Charge and is important in this highly personalized therapy for patients with cancer. Data presented here highlight the ability of this new manufacturing process to preserve unique stem-like T cells, which are critical for achieving responses at doses lower than those used for traditionally manufactured CAR T cells. Of note, patients who achieved CRs with YTB323 were shown to have an increased presence of younger memory T cells in the YTB323 final product that persisted during the peak expansion phase, further underlining the importance of retaining these less-differentiated T cells in a CAR-T product. It is unknown if preserving T-cell stemness may prolong YTB323 persistence, but future analyses with longer follow-up may shed light on this question. Thus, YTB323 merits continued exploration as a therapy for the treatment of patients with r/r DLBCL.

METHODS

CAR T-cell Manufacturing

Using the novel T-Charge manufacturing platform, T cells were enriched from healthy donor (preclinical studies) and patient (clinical trial) leukapheresis, followed by activation and transduction with a lentiviral vector encoding for the same CD19-targeting CAR construct used for tisagenlecleucel (13). After a short culture period, CAR T cells were harvested, washed, and formulated in <2 days (YTB323; Fig. 1). Following successful clinical manufacturing, quality assurance assays to assess cell viability, dose, and vector copy number were performed before the product was ready to administer. For preclinical studies using traditional manufacturing, T cells were enriched from the same healthy donor leukapheresis, activated, and transduced with an identical lentiviral vector. CAR T cells were then expanded for 9 to 11 days before being washed and formulated (CTL*019; Fig. 1).

Preclinical Development of YTB323

YTB323* In Vitro *Assessments. Leukapheresis material and YTB323 and CTL*019 products were analyzed by flow cytometry (Supplementary Fig. S10A) and scRNA-seq. CAR T-cell products were assessed in T-cell functional assays *in vitro*. A coculture model for the *in vitro* investigation of IL2 and IFNγ induction potential by CAR T cells was previously described (28). Briefly, coculture experiments were performed with a pre–B-ALL cell line (NALM6, CRL-3273), a CD19-knockout variant of NALM6 (NALM6-19KO), a DLBCL line (TMD8), or without cancer cells (T cells alone). The persistence and cytotoxic potential of YTB323 and CTL*019 were compared via repetitive stimulation with a red fluorescent protein (RFP)–labeled NALM6 ALL cell line. NALM6-RFP cells were cocultured with CTL*019 or YTB323 at various effector:target ratios. Media with fresh cancer cells were replaced (T cells were left behind) shortly after clearance of previous stimulation.

YTB323* In Vivo *Assessments. CAR T-cell products were assessed for antitumor activity and expansion *in vivo* in immunodeficient NSG mice inoculated with a pre–B-ALL cell line NALM6 (CRL-3273) expressing the luciferase reporter gene (NALM6-Luc) at 1×10^6 cells. All mouse experiments were conducted under protocol 20IMO001 approved by the Novartis Institutes for BioMedical Research Institutional Animal Care and Use Committee. On day 7 after tumor inoculation, mice were randomized and treated with YTB323 or CTL*019 at three different doses, with untransduced T cells as a negative control. YTB323 was dosed at 0.1×10^6, 0.25×10^6, and 1×10^6 viable CAR$^+$ T cells, and CTL*019 was dosed at 0.2×10^6, 0.5×10^6, and 2×10^6 viable CAR$^+$ T cells. The untransduced T-cell dose reflected the total T-cell dose of the respective CAR dose for YTB323 and CTL*019. Mice were imaged twice weekly to monitor tumor engraftment. Bioluminescent imaging was performed using a PerkinElmer IVIS Spectrum, and images were analyzed with Living Image 4.7.3 software. Blood samples were taken, and the expansion of CAR$^+$ T cells was analyzed by flow cytometry at 4, 7, 14, 21, and 28 days after CAR T-cell injection (Supplementary Fig. S10B). To assess *in vivo* expansion, cellular kinetic parameters of C_{max} and $AUC_{0\text{–}21d}$ after T-cell injection were calculated at different doses for YTB323 and CTL*019 in Phoenix 6.4. AUC was calculated through day 21 because CAR T-cell kinetics at later time points were perturbed by the onset of xenogeneic graft-versus-host–driven T-cell proliferation.

Clinical Studies

Trial Design and Patients. Based on preclinical evidence, the safety and efficacy of YTB323 are currently being investigated in a first-in-human, phase I, multicenter study in adult patients with B-cell malignancies, including r/r DLBCL, r/r ALL, and CLL/small lymphocytic leukemia (NCT03960840). The study protocol and statistical analysis plan are included in the Supplementary Information. Before initiation of the trial, the investigator/institution obtained approval from the Institutional Review Board/Independent Ethics Committee for the trial protocol, written informed consent forms, consent form updates, patient recruitment procedures (e.g., advertisements), and any other written information to be provided to patients. Before enrollment, all patients were required to sign a written informed consent form. Results presented here focus on the DLBCL cohort and represent an interim data cut to drive dose decisions for the expansion phase of the trial. Eligible patients were adults (≥18 years old) with measurable disease at screening and r/r DLBCL after ≥2 lines of prior therapy, including HSCT. An Eastern Cooperative Oncology Group performance status of 0 or 1 at screening and leukapheresis material of nonmobilized cells accepted for manufacturing was required. Eligible patients were considered suitable by the investigator to undergo the protocol-prescribed lymphodepletion regimen. Patients were excluded if they had prior CD19-directed therapy, prior administration of a genetically modified cellular product, or prior allogeneic HSCT. Patients with DLBCL with Burkitt-like features and primary central nervous system lymphoma were also excluded.

After providing written informed consent, screened patients underwent leukapheresis for autologous T-cell collection. Enrollment in the trial required patients to have a minimum number of T cells recovered during leukapheresis. The final YTB323 product release specifications included cell viability and B-cell, T-cell, and vector copy number. Before infusion, patients received lymphodepleting chemotherapy of either fludarabine (30 mg/m^2) and cyclophosphamide (500 mg/m^2) daily for 3 days or bendamustine (90 mg/m^2) daily for 2 days. Patients from 21 sites across the United States, Australia, Austria, France, Italy, Japan, and Spain received single-dose YTB323 at DL1 (2.5×10^6 CAR$^+$ viable T cells) or DL2 (12.5×10^6 CAR$^+$ viable T cells). Bridging therapy prior to YTB323 was optional and based on the investigator's decision. Study treatment was discontinued based on participant/guardian decision, pregnancy, and safety risks.

Data Analysis. The full analysis and safety sets comprise all patients who received YTB323. Patients were analyzed according to the dose of YTB323 received, defined as the dose of YTB323 taken on study day 1. The pharmacokinetic analysis set for YTB323 includes all patients who received YTB323 with at least one measurable concentration. Data were summarized using descriptive statistics (continuous data) and/or contingency tables (categorical data presented as frequencies and percentages) for demographic and baseline characteristics and efficacy, safety, cellular kinetic/pharmacokinetic, and pharmacodynamic measurements.

Endpoints. Primary endpoints are the incidence and nature of DLTs in the first 28 days after YTB323 infusion and the incidence and severity of AEs and serious AEs after YTB323 infusion to determine a recommended phase II dose, as well as the manufacturing success rate to evaluate the feasibility of the manufacturing process. Secondary endpoints are *in vivo* cellular kinetics, ORR by local investigator assessment, duration of response, and OS.

Assessments. Efficacy was assessed using the Chesson Response Criteria and Lugano classification (29, 30). ORR was defined as the proportion of patients with a best overall response of CR or PR. CR, PR, and ORR were assessed at 1, 3, 6, and 12 months. Best overall response was defined as the best overall disease response recorded from the start of treatment until PD or the start of new anticancer therapy, whichever comes first. Duration of response was defined as the time from achievement of CR/PR or to first documented disease progression or death due to DLBCL. OS was defined as the time from the date of start of treatment to the date of death due to any cause.

Disease and response assessment (including PET-CT) were performed at screening, on day 28 (±1 day), at months 3 (±7 days), 6, 9, 12, 18, 24 (±14 days), and every 12 months until relapse. Bone marrow was evaluated by biopsy/aspirate at screening for all patients, at months 3 (±7 days), 6, 12, 24 (±14 days), and every 12 months until relapse if bone marrow was positive for lymphoma at screening. For patients receiving bridging chemotherapy, a PET-CT scan was obtained after the last cycle of chemotherapy and within 4 weeks from YTB323 infusion. For patients who did not receive bridging and have more than 8 weeks between screening and YTB323 infusion, a repeat PET-CT scan is required.

YTB323 concentrations in peripheral blood were assessed by quantitative polymerase chain reaction (qPCR) for YTB323 transgene levels (copies/μg of DNA) and by flow cytometry for YTB323-transduced cells (percentage of CAR^+ cells in $CD3^+$ cells). AEs were assessed according to the Medical Dictionary for Regulatory Activities (MedDRA) v24.0 and CTCAE v5.0, except for the grading of CRS. CRS events were graded per Lee and colleagues (16) and ASTCT consensus grading scales, and NAR, including ICANS, were graded according to CTCAE v5.0.

Flow Cytometric Analysis. Leukapheresis and final cell product samples were collected in sodium heparin vacutainer tubes and frozen. Immunophenotyping was performed starting with approximately 2×10^7 total white blood cells (WBC). The WBC gate was adjusted to include WBCs and exclude any red blood cells, apoptotic cells, and debris by avoiding the cluster of cells with low forward and side scatter. A 12-color flow cytometry assay was performed using the BD LSRFortessa X-20 instrument to determine frequencies of T-cell phenotypes—naive/T_{SCM}, central memory, effector memory, exhausted/senescent—as well as checkpoint expression within $CD4^+$ and $CD8^+$ T cells. Phenotypic markers used to identify and characterize T cells included viability, CD3, CD45RA, CCR7, PD-1, CD45RO, TIM3, CD28, CD27, CD4, CD8, LAG3, and a custom anti-CART19. For JULIET patients, T cells were characterized by viability, CD3, CD8, CD45RA, CCR7, CD27, CD45RO, CD4, and a custom anti-CART19 (4). Because the flow cytometry panels for the present YTB323 study differed in cell marker content compared with those used in the JULIET study, no formal comparisons were performed. Plots correlating flow cytometry results with clinical outcome are only descriptive given the small number of patients with PD, and no formal statistical hypothesis testing was conducted.

Processing of Bulk RNA-seq Data. Total RNA was purified according to the manufacturer's instructions (Qiagen), and integrity was verified with an Agilent TapeStation. Preparation for sequencing was performed with a TruSeq RNA v2 prep kit (Illumina). Captured libraries were pooled, each having a unique adapter index sequence, and applied to a sequencing flow cell. The flow cell then underwent cluster amplification and massively parallel sequencing by synthesis using standard approaches (Illumina). Library pooling and flow cell loading were coordinated to target a median 50 million sequencing reads per library. Reads were aligned to the reference human genome (build hg19) in STAR (31). Mapped reads were assembled into transcripts, and transcript abundances were estimated and normalized using Cufflinks (32). Finally, high-throughput sequencing analysis was used to count the number of reads mapping to each gene (33). Data normalization for differential expression analysis was carried out using the edgeR R package (34).

Processing of scRNA-seq Data. 10x Genomics Chromium was used to isolate single cells from cryopreserved cells. Between 10,000 and 20,000 cells per sample were inputted into the Chromium instrument, targeting data generation between 5,000 and 10,000 cells. 10x Genomics single-cell 5′ library construction was conducted. The final amplified libraries were pooled, each having a unique adapter index sequence, and applied to a sequencing flow cell. The flow cell underwent cluster amplification and massively parallel sequencing by synthesis using standard approaches (Illumina). Library pooling and flow cell loading were coordinated to target a median coverage of 50,000 reads per cell. The raw sequencing data were processed through 10x Genomics CellRanger, mkfastq, count, and aggr for the 5′ gene expression assay. The human reference genome is based on GRCh38. After CellRanger was run, additional quality control criteria removed droplets that met any of the three conditions: percent of mitochondrial unique molecular identifiers >15%, number of genes detected <200, and number of unique molecular identifiers <800. SoupX v1.4.5 was used to estimate ambient RNA for each sample, and the Seurat R package was used for batch effect check and data normalization. Cell-type annotation of the processed single-cell data were performed using the R Symphony package with the Genevestigator peripheral blood mononuclear cell-type reference (35) along with manual annotation of regulatory, activated, exhausted, and activated exhausted T cells and the removal of red blood cells from the data. A Treg was defined as $FOXP3^+$, $IKZ2^+$, $IL2^-$, and IFNγ-low. An activated T cell was defined as a cell falling into a CD25-high cluster and not meeting the definition of a Treg. An exhausted T cell was defined as expressing at least two of the following three genes: *PDCD1, LAG3,* and/or *HAVCR2*. An activated exhausted T cell (Act_Exh T-cell) was defined as meeting both activated and exhausted T-cell criteria.

Statistical Analysis. To guide dose escalation, a two-parameter Bayesian logistic regression model was used. The dose used in the model was the square root transformation of the actual CAR^+ viable T cells. The Bayesian logistic regression model incorporates all the available DLT information accumulated across all dose cohorts during the first 28 days of the DLT evaluation period. ORR during the study, as well as ORR and CR rates at selected time points (months 3, 6, and 9), was summarized along with 95% exact Clopper–Pearson confidence intervals (CI). Further follow-up is required to develop a meaningful duration of response and OS estimates.

Cellular kinetics parameters were determined using a noncompartmental analysis in Phoenix 6.4. Parameters of C_{max}, T_{max}, and

AUC_{0-28d} were calculated to assess CAR T-cell expansion. Differences in $CD4^+$ and $CD8^+$ subsets between the final product and leukapheresis from flow cytometry were determined, and 95% CIs were estimated from a Student *t* distribution. Differences in stemness between the final product and leukapheresis were assessed from flow cytometry analysis of T-cell subsets, bulk RNA-seq, and scRNA-seq using single-sample gene set scores.

The proportion of cells in every identified cell type was calculated for each sample from the scRNA-seq data. For each cell type, the difference in medians between CRs and PDs was calculated for the final product and leukapheresis samples. Rare subtypes found in <2% of all samples were removed from each analysis.

Differential gene expression of scRNA-seq data was performed using the Seurat FindMarkers function. Differential gene expression of bulk RNA-seq data was performed using edgeR. The top 25 genes upregulated in each group were selected for gene set overlap analysis using the MSigDB Compute Overlaps function with a selection of T-cell relevant gene sets from the C2 and ImmuneSigDB gene sets.

Data Sharing Statement. Novartis is committed to sharing with qualified external researchers access to patient-level data and supporting clinical documents from eligible studies. These requests are reviewed and approved by an independent review panel on the basis of scientific merit. All data provided are anonymized to respect the privacy of patients who have participated in the trial in line with applicable laws and regulations. The data availability of these trials is according to the criteria and process described at www.clinicalstudydatarequest.com.

Authors' Disclosures

M.J. Dickinson reports grants and personal fees from Novartis, Gilead, Roche, AbbVie, and Genmab, and personal fees from Kite, Bristol Myers Squibb, NKARTA, and Adicet Bio during the conduct of the study. P. Barba reports other support from Jazz Pharmaceuticals, Nektar, Pierre Fabre, Miltenyi Biomedicine, Novartis, Allogene, Bristol Myers Squibb, Incyte, and Kite/Gilead outside the submitted work. U. Jager reports grants and personal fees from Novartis during the conduct of the study, as well as personal fees from Bristol Myers Squibb, Gilead, Miltenyi, Janssen, and Roche outside the submitted work. N.N. Shah reports personal fees from Novartis during the conduct of the study; personal fees from Kite Pharma, Miltenyi Biotec, and Bristol Myers Squibb/Juno outside the submitted work; and advisory board participation for Incyte, Seattle Genetics, TG Therapeutics, Umoja, Janssen, Epizyme, and Loxo/Lilly. N. Boissel reports personal fees from Novartis, Amgen, Pfizer, and Servier outside the submitted work. A. Bondanza reports personal fees from Novartis during the conduct of the study, as well as a patent for USPA 62/726,155 pending. L. Mariconti reports other support (employee and shareholder) from Novartis during the conduct of the study, as well as other support (employee and shareholder) from Novartis outside the submitted work. A.-L. Marchal reports other support (employee and shareholder) from Novartis during the conduct of the study, as well as other support (employee and shareholder) from Novartis outside the submitted work. J. Yang reports other support from Novartis outside the submitted work. A. Sohoni reports a patent for a novel autologous CAR-T therapy, YTB323, pending to the World Intellectual Property Organization (WIPO). L.M. Treanor is an employee of, is a current holder of stock options with, and holds patents with Novartis Institutes for BioMedical Research. E.J. Orlando reports employment with Novartis. J. Davis reports personal fees from Novartis Pharmaceuticals Corporation during the conduct of the study, as well as personal fees from Novartis Pharmaceuticals Corporation outside the submitted work. B. Engels reports other support from Novartis outside the submitted work; a patent for methods of making CAR-expressing cells pending; and ended employment with Novartis, is a current holder of stocks in, and holds patents with Novartis Institutes for BioMedical Research. L. Moutouh-de Parseval reports personal fees and other support from Novartis outside the submitted work. J.L. Brogdon reports employment with, is a current holder of stock options with, and holds patents with Novartis Institutes for BioMedical Research. M. Moschetta reports other support from Novartis Pharma AG during the conduct of the study, as well as other support from Novartis Pharma AG outside the submitted work. I.W. Flinn reports other support from AbbVie, BeiGene, Centruy Therapeutics, Genentech, Genmab, Hutchison MediPharma, InnoCare Pharma, Kite Pharma, Myeloid Therapeutics, Novartis, Secura Bio, Servier Pharmaceuticals, TG Therapeutics, Vincerx Pharma, and Xencor during the conduct of the study, as well as grants from AbbVie, Acerta Pharma, Agios, ArQule, AstraZeneca, BeiGene, Biopath, Bristol Myers Squibb, CALIBR, Celgene, CALGB, City of Hope National Medical Center, Constellation Pharmaceuticals, Curis, CTI Biopharma, Epizyme, Fate Therapeutics, Forty Seven, Genentech, Gilead Sciences, InnoCare Pharma, IGM Biosciences, Incyte, Infinity Pharmaceuticals, Janssen, Kite Pharma, Loxo, Marker Therapeutics, Merck, Millennium Pharmaceuticals, Rhizen Pharmaceuticals, MorphoSys, Myeloid Therapeutics, Novartis, Nurix Pharma, Tessa Therapeutics, TG Therapeutics, Trillium Therapeutics, Triphase Research and Development Corp., Unum Therapeutics, Verastem, Vincerx Pharma, and 2seventy Bio outside the submitted work. No disclosures were reported by the other authors.

Authors' Contributions

M.J. Dickinson: Conceptualization, investigation, writing–review and editing. **P. Barba:** Conceptualization, investigation, writing–review and editing. **U. Jager:** Conceptualization, investigation, writing–review and editing. **N.N. Shah:** Investigation, writing–review and editing. **D. Blaise:** Investigation, writing–review and editing. **J. Briones:** Investigation, writing–review and editing. **L. Shune:** Investigation, writing–review and editing. **N. Boissel:** Investigation, writing–review and editing. **A. Bondanza:** Conceptualization, writing–review and editing. **L. Mariconti:** Formal analysis, writing–review and editing. **A.-L. Marchal:** Formal analysis, writing–review and editing. **D.S. Quinn:** Formal analysis, writing–review and editing. **J. Yang:** Formal analysis, writing–review and editing. **A. Price:** Formal analysis, writing–review and editing. **A. Sohoni:** Formal analysis, writing–review and editing. **L.M. Treanor:** Formal analysis, writing–review and editing. **E.J. Orlando:** Formal analysis, writing–review and editing. **J. Mataraza:** Formal analysis, writing–review and editing. **J. Davis:** Formal analysis, writing–review and editing. **D. Lu:** Formal analysis, writing–review and editing. **X. Zhu:** Formal analysis, writing–review and editing. **B. Engels:** Formal analysis, writing–review and editing. **L. Moutouh-de Parseval:** Formal analysis, writing–review and editing. **J.L. Brogdon:** Formal analysis, supervision, writing–review and editing. **M. Moschetta:** Conceptualization, writing–review and editing. **I.W. Flinn:** Conceptualization, investigation, writing–review and editing.

Acknowledgments

The study was sponsored and designed by Novartis Pharmaceuticals Corporation and approved by the institutional review board at each participating institution. Data were analyzed and interpreted by the sponsor and authors. All of the authors reviewed the manuscript and approved of the final version before submission. The authors vouch for the data, analyses, and adherence to the study to the protocol. Medical writing support was provided by Jacqueline R. Ward, PhD, and Kymberleigh Romano, PhD, of Healthcare Consultancy Group and funded by Novartis Pharmaceuticals Corporation. The authors thank Xiaoyan Li and Matt Niederst for their contributions to the development and execution of the tumor stress test *in vitro* and

Gina Trabucco for her contribution to the analysis of flow cytometry data. Figure 2A and D were originally published in *Blood*. Engels B, et al. *Blood* 2021;138(suppl 1): Abstract 2848. © 2021 the American Society of Hematology.

The publication costs of this article were defrayed in part by the payment of publication fees. Therefore, and solely to indicate this fact, this article is hereby marked "advertisement" in accordance with 18 USC section 1734.

Note

Supplementary data for this article are available at Cancer Discovery Online (http://cancerdiscovery.aacrjournals.org/).

Received November 11, 2022; revised February 21, 2023; accepted May 23, 2023; published first May 30, 2023.

REFERENCES

1. Abramson JS, Palomba ML, Gordon LI, Lunning MA, Wang M, Arnason J, et al. Lisocabtagene maraleucel for patients with relapsed or refractory large B-cell lymphomas (TRANSCEND NHL 001): a multicentre seamless design study. Lancet 2020;396:839–52.
2. Locke FL, Ghobadi A, Jacobson CA, Miklos DB, Lekakis LJ, Oluwole OO, et al. Long-term safety and activity of axicabtagene ciloleucel in refractory large B-cell lymphoma (ZUMA-1): a single-arm, multicentre, phase 1–2 trial. Lancet Oncol 2019;20:31–42.
3. Neelapu SS, Locke FL, Bartlett NL, Lekakis LJ, Miklos DB, Jacobson CA, et al. Axicabtagene ciloleucel CAR T-cell therapy in refractory large B-cell lymphoma. N Engl J Med 2017;377:2531–44.
4. Schuster SJ, Bishop MR, Tam CS, Waller EK, Borchmann P, McGuirk JP, et al. Tisagenlecleucel in adult relapsed or refractory diffuse large B-cell lymphoma. N Engl J Med 2019;380:45–56.
5. Schuster SJ, Svoboda J, Chong EA, Nasta SD, Mato AR, Anak O, et al. Chimeric antigen receptor T cells in refractory B-cell lymphomas. N Engl J Med 2017;377:2545–54.
6. Ghassemi S, Nunez-Cruz S, O'Connor RS, Fraietta JA, Patel PR, Scholler J, et al. Reducing ex vivo culture improves the antileukemic activity of chimeric antigen receptor (CAR) T cells. Cancer Immunol Res 2018;6:1100–9.
7. Gattinoni L, Lugli E, Ji Y, Pos Z, Paulos CM, Quigley MF, et al. A human memory T cell subset with stem cell-like properties. Nat Med 2011;17:1290–7.
8. Gattinoni L, Speiser DE, Lichterfeld M, Bonini C. T memory stem cells in health and disease. Nat Med 2017;23:18–27.
9. Fraietta JA, Lacey SF, Orlando EJ, Pruteanu-Malinici I, Gohil M, Lundh S, et al. Determinants of response and resistance to CD19 chimeric antigen receptor (CAR) T cell therapy of chronic lymphocytic leukemia. Nat Med 2018;24:563–71.
10. Ghassemi S, Durgin JS, Nunez-Cruz S, Patel J, Leferovich J, Pinzone M, et al. Rapid manufacturing of non-activated potent CAR T cells. Nat Biomed Eng 2022;6:118–28.
11. Arcangeli S, Bove C, Mezzanotte C, Camisa B, Falcone L, Manfredi F, et al. CAR T-cell manufacturing from naive/stem memory T-lymphocytes enhances antitumor responses while curtailing cytokine release syndrome. J Clin Invest 2022;132:e150807.
12. Maude SL, Laetsch TW, Buechner J, Rives S, Boyer M, Bittencourt H, et al. Tisagenlecleucel in children and young adults with B-cell lymphoblastic leukemia. N Engl J Med 2018;378:439–48.
13. Engels B, Zhu X, Yang J, Price A, Sohoni A, Stein AM, et al. Preservation of T-cell stemness with a novel expansionless CAR-T manufacturing process, which reduces manufacturing time to less than two days, drives enhanced CAR-T cell efficacy. Blood 2021;138 Suppl 1:2848.
14. Tyagarajan S, Spencer T, Smith J. Optimizing CAR-T cell manufacturing processes during pivotal clinical trials. Mol Ther Methods Clin Dev 2020;16:136–44.
15. Boise LH, Minn AJ, Noel PJ, June CH, Accavitti MA, Lindsten T, et al. CD28 costimulation can promote T cell survival by enhancing the expression of Bcl-XL. Immunity 1995;3:87–98.
16. Lee DW, Gardner R, Porter DL, Louis CU, Ahmed N, Jensen M, et al. Current concepts in the diagnosis and management of cytokine release syndrome. Blood 2014;124:188–95.
17. Lee DW, Santomasso BD, Locke FL, Ghobadi A, Turtle CJ, Brudno JN, et al. ASTCT consensus grading for cytokine release syndrome and neurologic toxicity associated with immune effector cells. Biol Blood Marrow Transplant 2019;25:625–38.
18. YESCARTA (axicabtagene ciloleucel) [prescribing information]; [about 2 screens]. Santa Monica (CA): Kite Pharma Inc. [updated 2022 Apr 1; cited 2017 Nov 2]. Available from: https://www.fda.gov/vaccines-blood-biologics/cellular-gene-therapy-products/yescarta-axicabtagene-ciloleucel.
19. BREYANZI (lisocabtagene maraleucel) [prescribing information]; [about 2 screens]. Bothell (WA): Juno Therapeutics, Inc., a Bristol-Myers Squibb Company [updated 2022 Jun 24; cited 2021 Feb 5]. Available from: https://www.fda.gov/vaccines-blood-biologics/cellular-gene-therapy-products/breyanzi-lisocabtagene-maraleucel.
20. Flinn IW, Jaeger U, Shah NN, Blaise D, Briones J, Shune L, et al. A first-in-human study of YTB323, a novel, autologous CD19-directed CAR-T cell therapy manufactured using the novel T-charge TM platform, for the treatment of patients (pts) with relapsed/refractory (r/r) diffuse large B-cell lymphoma (DLBCL). Blood 2021;138 Suppl 1:740.
21. Awasthi R, Pacaud L, Waldron E, Tam CS, Jager U, Borchmann P, et al. Tisagenlecleucel cellular kinetics, dose, and immunogenicity in relation to clinical factors in relapsed/refractory DLBCL. Blood Adv 2020;4:560–72.
22. Ivanova NB, Dimos JT, Schaniel C, Hackney JA, Moore KA, Lemischka IR. A stem cell molecular signature. Science 2002;298:601–4.
23. Jerby-Arnon L, Shah P, Cuoco MS, Rodman C, Su MJ, Melms JC, et al. A cancer cell program promotes T cell exclusion and resistance to checkpoint blockade. Cell 2018;175:984–97.
24. Wong DJ, Liu H, Ridky TW, Cassarino D, Segal E, Chang HY. Module map of stem cell genes guides creation of epithelial cancer stem cells. Cell Stem Cell 2008;2:333–44.
25. Rodrigues M, Duran E, Eschgfaeller B, Kuzan D, Habucky K. Optimizing commercial manufacturing of tisagenlecleucel for patients in the US: a 4-year experiential journey. Blood 2021;138 Suppl 1:1768.
26. Rodrigues M, Kuzan D, Yallouridis A, Saffar JM, Eschgfaeller B. Commercial manufacturing experience of tisagenlecleucel in Europe: >3 years journey. Bone Marow Transplant 2022;57 Suppl 1:144. Abstract nr P079.
27. Barba P, Kwon M, Briones J, Jaeger U, Bachy E, Blaise D, et al. YTB323 (rapcabtagene autoleucel) demonstrates durable efficacy and a manageable safety profile in patients with relapsed/refractory diffuse large B-cell lymphoma: phase I study update. In: Proceedings of the 64th American Society of Hematology Annual Meeting and Exposition; 2022 Dec 10–13; New Orleans, LA [cited 2022 Dec 11]. Abstract nr 439. Available from: https://www.medicalcongress.novartisoncology.com/ASH22/CART/pdf/Barba_Oral_439.pdf.
28. Norelli M, Camisa B, Barbiera G, Falcone L, Purevdorj A, Genua M, et al. Monocyte-derived IL-1 and IL-6 are differentially required for cytokine-release syndrome and neurotoxicity due to CAR T cells. Nat Med 2018;24:739–48.
29. Cheson BD, Fisher RI, Barrington SF, Cavalli F, Schwartz LH, Zucca E, et al. Recommendations for initial evaluation, staging, and response assessment of Hodgkin and non-Hodgkin lymphoma: the Lugano classification. J Clin Oncol 2014;32:3059–68.
30. Barrington SF, Mikhaeel NG, Kostakoglu L, Meignan M, Hutchings M, Mueller SP, et al. Role of imaging in the staging and response assessment of lymphoma: consensus of the International Conference on Malignant Lymphomas Imaging Working Group. J Clin Oncol 2014;32:3048–58.
31. Dobin A, Davis CA, Schlesinger F, Drenkow J, Zaleski C, Jha S, et al. STAR: ultrafast universal RNA-seq aligner. Bioinformatics 2013;29:15–21.
32. Trapnell C, Roberts A, Goff L, Pertea G, Kim D, Kelley DR, et al. Differential gene and transcript expression analysis of RNA-seq experiments with TopHat and Cufflinks. Nat Protoc 2012;7:562–78.

33. Anders S, Pyl PT, Huber W. HTSeq–a Python framework to work with high-throughput sequencing data. Bioinformatics 2015;31:166–9.
34. Robinson MD, McCarthy DJ, Smyth GK. edgeR: a Bioconductor package for differential expression analysis of digital gene expression data. Bioinformatics 2010;26:139–40.
35. Zheng L, Qin S, Si W, Wang A, Xing B, Gao R, et al. Pan-cancer single-cell landscape of tumor-infiltrating T cells. Science 2021;374:abe6474.
36. Ramalho-Santos M, Yoon S, Matsuzaki Y, Mulligan RC, Melton DA. "Stemness": transcriptional profiling of embryonic and adult stem cells. Science 2002;298:597–600.